

# A Robust Approach for Breast Cancer Classification from DICOM Images

**Thanh-Nghia Nguyen**

Department of Industrial Electronics and Biomedical Engineering, Ho Chi Minh City University of Technology and Education, Ho Chi Minh City, Vietnam  
nghiant@hcmute.edu.vn

**Thanh-Tam Nguyen**

Department of Industrial Electronics and Biomedical Engineering, Ho Chi Minh City University of Technology and Education, Ho Chi Minh City, Vietnam  
tamnt.ncs@hcmute.edu.vn

**Thanh-Hai Nguyen**

Department of Industrial Electronics and Biomedical Engineering, Ho Chi Minh City University of Technology and Education, Ho Chi Minh City, Vietnam  
nthai@hcmute.edu.vn (corresponding author)

**Ba-Viet Ngo**

Department of Industrial Electronics and Biomedical Engineering, Ho Chi Minh City University of Technology and Education, Ho Chi Minh City, Vietnam  
vietnb@hcmute.edu.vn

Received: 13 March 2025 | Revised: 3 April 2025 | Accepted: 9 April 2025

Licensed under a CC-BY 4.0 license | Copyright (c) by the authors | DOI: <https://doi.org/10.48084/etasr.10931>

## ABSTRACT

The number of breast cancer patients is rapidly increasing worldwide, with Asia currently accounting for 45% of global breast cancer cases. In addition, the number of breast cancer cases is expected to increase by 21.0%, and the mortality rate is projected to increase by 27.8% during the 2020-2030 period. This paper proposes a method for classifying breast cancer from Digital Imaging and Communications in Medicine (DICOM) images. In particular, an image segmentation technique was developed for extracting the breast region from DICOM images of varying sizes. The extracted images were then enhanced using multiple augmentation techniques to improve classification performance. Finally, a deep learning network was applied to classify breast cancer from the processed DICOM images. The VinDr-Mammo dataset was used to evaluate the effectiveness of the proposed method, and the experimental results showed an accuracy of 81.45%, demonstrating that the proposed approach is highly suitable for breast cancer detection and classification.

**Keywords**-breast cancer classification; deep learning; DICOM image preprocessing; image augmentation; ResNet50

## I. INTRODUCTION

Currently, the number of Breast Cancer (BC) patients is rapidly increasing worldwide each year. According to statistics from the Global Cancer Organization (GLOBOCAN), in 2022, more than 2.3 million women were diagnosed with BC, with almost 670,000 deaths [1]. In Asia, the region accounts for 45% of global BC cases, and the number of cases is projected to increase by 21.0%, while the mortality rate is expected to increase by 27.8% during the 2020-2030 period [2]. In Vietnam alone, approximately 21,555 new cases and 9,345 deaths are

recorded annually, accounting for 25.8% of all cancers in women [3]. BC is currently the second most common cancer among women worldwide. Early classification and treatment can significantly improve outcomes. Studies in Asian countries have shown a 5-year survival rate ranging from 56.5% to 86.7%.

In Vietnam, patients with BC diagnosed at an early stage can have a five-year survival rate of up to 90%. Moreover, a recent study on women under 35 years of age revealed that the overall 10-year survival rate for early-stage cases exceeds 80% [3]. In practice, physicians face challenges in classifying and

diagnosing BC due to difficulties in interpreting medical images (such as identifying tumors and calcifications). Furthermore, the need to analyze a large number of breast images daily can impact diagnostic accuracy. Therefore, developing a supportive system for BC diagnosis is essential. Such a system would help physicians analyze and interpret mammographic images more effectively, enabling timely and appropriate treatment decisions.

With the advancement of Artificial Intelligence (AI), Deep Learning (DL) techniques have been used effectively in BC classification, enabling early diagnosis and, thus, increasing patient survival rates [4-6]. Several recent studies have employed DL methods to classify BC using different imaging approaches. In [7], a VGG16 network model was combined with transfer learning to extract features from the BreakHis histopathological image dataset, achieving an accuracy of 89%. In [8], a model based on k-means, GMM, and CNN, utilizing Region Of Interest (ROI) for feature extraction, achieved an accuracy of 95.8%. The study in [9] focused on Lloyd's algorithm for clustering combined with CNN for classification, achieving an accuracy of 96%. These studies demonstrate the effectiveness of DL applications in BC classification.

TABLE I. A SUMMARY OF PREPROCESSING AND DEEP LEARNING METHODS FOR BC CLASSIFICATION

Ref.	Dataset (Output classes)	Preprocessing method	Model	Result
[10]	The NYU BC screening dataset V1.0 with over 1,000,000 images (benign and malignant)	Image normalization, data augmentation.	Custom ResNet-based CNN	AUC = 0.895
[11]	Assessment on the EDA dataset with 3,002 mammographic images (benign and malignant)	Removal of low-variance features, univariate feature selection, recursive feature elimination.	CNN-BCC	High efficiency
[12]	Breast ultrasound images, MIAS, Mini-DDSM,	Wiener filtering, total variation filtering, image segmentation.	ViT, U-KAN	ViT accuracy: 99.3%, U-KAN: 93.3% accuracy
[13]	3,002 digital mammography images (benign and malignant)	CNN deep feature extraction, feature fusion.	CNN-ELM hybrid	Improved classification accuracy

Table I provides a comparative analysis of some research studies focused on BC classification using various Machine Learning (ML) and DL approaches. Each study employed different preprocessing techniques, such as image normalization, feature selection, filtering, and contrast enhancement, to improve data quality prior to classification. The classification methods range from traditional ML models [11] to advanced DL models (e.g., CNN, Vision Transformer, U-Net, and Extreme Learning Machine) [10, 12, 13]. The datasets used include mammographic images from large-scale screening examinations (eg, more than 200,000 mammograms in [10]), as well as multiple public datasets (BreastDM, MIAS, BUSI, BreakHis, DDSM) [12]. The classification outputs focus mainly on distinguishing benign and malignant tumors, with some studies extending to subtype classification [12]. The results indicate that DL models generally outperform

traditional ML approaches, with CNN-based and transformer models achieving the highest accuracies (up to 99.3% in some cases). However, generalizability and computational efficiency remain challenging, highlighting the need for further DL systems to enhance the accuracy of BC classification. This comparative study underscores the rapid advancements in AI-driven BC classification and the potential of DL to improve diagnostic accuracy and support radiologists in clinical settings.

With the above statistics, BC classification plays a crucial role in current research. This paper proposes a robust method for classifying BC based on DICOM images. In particular, a DICOM image preprocessing method is applied to enhance image quality and improve classification performance. A DL network is then utilized to classify the DICOM images after preprocessing, as well as distinguishing different types of BC. The research results aim to help physicians diagnose early BC, enabling better treatment for patients. The main contributions of this study involve:

- Developing a method for extracting breast regions from DICOM images of various sizes captured by different imaging devices,
- Building a DL system for BC classification using DICOM images,
- Identifying multiple types of BC images with high accuracy.

## II. MATERIAL AND METHOD

To classify different types of BC, images need to be processed and fed into a classification network. This section presents a proposed system for BC classification and the core theoretical concepts utilized.

### A. Proposed Framework for BC Classification

The proposed system for BC classification, shown in Figure 1, consists of the following blocks: BC image data, image preprocessing, DL network for classification, and classification results. In particular, BC images are a DICOM dataset of breast images, which are automatically preprocessed by cropping and resizing. Data augmentation is applied to increase the number of images in the four different classes of the dataset for balancing their number of images. The training and testing blocks are designed for training and classifying different BC types. Finally, the classification results provide an evaluation of the proposed system.

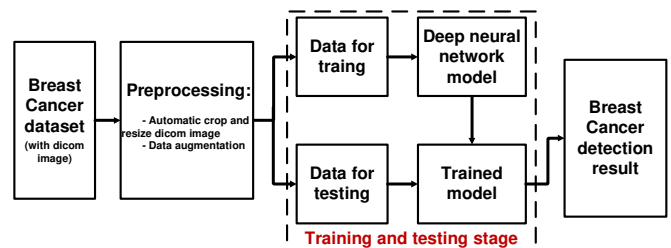


Fig. 1. Block diagram of the proposed method for BC classification.

### B. Breast Cancer Dataset

This study used the VinDr-Mammo image dataset [14], which contains BC images in DICOM format, as described in Table II. DICOM images not only provide high-quality medical imaging but also store important patient information and technical parameters of the imaging device, such as patient name, age, imaging date, imaging machine type, and specific technical details. This direct connection between medical images and patient information enhances the accuracy and efficiency of diagnosis and treatment. Each patient underwent imaging in multiple views: L-CC (Left Craniocaudal), L-MLO (Left Mediolateral Oblique), R-CC (Right Craniocaudal), and R-MLO (Right Mediolateral Oblique). An example illustration of a breast cancer patient includes images from L-CC, L-MLO, R-CC, and R-MLO views.

TABLE II. BREAST CANCER DATASET [14]

Class	Label	BI-RADS	Total
1	Mass	3, 4, and 5	1113
2	Calcification	3, 4, and 5	212
3	Architectural and Asymmetry	3, 4, and 5	390
4	Normal	1 and 2	18232

### C. DICOM Image Preprocessing

The VinDr-Mammo dataset was collected from multiple imaging devices, resulting in inconsistent image sizes. The dataset includes images captured from four different mammography machines: Mammomat Inspiration (image size: 3518×2800), Planmed Nuance (image size: 2812×2012), Giotto Image 3DL (image size: 3580×2812), and Giotto Class (image sizes: 3580×2531 and 3580×2543). The breast region in the images is often positioned to one side and occupies a relatively small area compared to the entire image frame. Therefore, preprocessing breast cancer images is essential. The preprocessing steps used in this study are described below.

### D. Otsu and Contours Methods for Classification of Image Boundaries

The Otsu method is used to automatically determine a threshold to distinguish between the background and the object in an image. After loading the image and converting it into a NumPy array for easier processing, if the image format is not the type of uint16, it is converted to it. Therefore, the dataset containing these images with different resolutions requires standardization to be in 16-bit format. For processing these images, the Otsu method is applied to construct the image histogram, which represents the number of pixels for each grayscale value from 0 to 65,535. For determining each threshold value, the Otsu method can calculate the proportion of pixels belonging to the background and object classes. Then, the probability of each grayscale level  $p(i)$  is determined, which divides the number of pixels at that grayscale level by the total number of pixels. Thus, the overall mean  $\mu_T$  of the whole image is calculated using the following formula:

$$\mu_T = \sum_{i=0}^{L-1} i * p(i) \quad (1)$$

where  $L$  is the total number of grayscale levels.

The mean of the background and object classes for each threshold  $k$  are calculated as follows:

$$\mu_B(k) = \frac{\sum_{i=0}^k i * p(i)}{\omega_B(k)} \quad (2)$$

$$\mu_F(k) = \frac{\sum_{i=k+1}^{L-1} i * p(i)}{\omega_F(k)} \quad (3)$$

where  $\omega_B(k)$  and  $\omega_F(k)$  are the weights of the background and object classes, respectively. Thus, the between-class variance  $\sigma_B^2(k)$  is calculated as follows:

$$\sigma_B^2(k) = \omega_F(k) * \omega_B(k) (\mu_B(k) - \mu_F(k))^2 \quad (4)$$

Comparing all threshold values  $k$  and calculating  $\sigma_B^2(k)$  for each threshold aims to determine the optimal threshold that reaches the maximum value. In addition, the output is a binary image, where pixels having values greater than the threshold are assigned the maximum value (65535), and the other pixels are assigned 0. From the obtained binary image, the contours method is used to classify the boundaries around objects in the image. Identifying contours can help to more accurately and efficiently distinguish objects from the background.

#### 1) Creating a Bounding Box and Cropping the Image

A bounding box technique and a common image annotation method were used to accurately crop the identified object. The bounding box creates a rectangular region around the target object. After detecting the object's shape using the contour method, a bounding box is generated for the largest contour in the image. The dimensions of the bounding box correspond to the height and width of the contour. The coordinates for cropping the image at the correct position can then be calculated, ensuring the mammogram is fully captured without distortion.

#### 2) Image Resizing Method

To ensure a uniform output size after cropping, the image is resized to 512×512 maintaining the original aspect ratio. If only one dimension is adjusted without preserving the aspect ratio, the image will be distorted. To avoid this distortion, it is crucial to calculate using a consistent scaling factor to both dimensions (width and height). The resizing process maintaining the original aspect ratio follows these steps:

- To calculate the scaling ratio for each height or width, the target size can be divided by using the original image size as follows:

$$h\_ratio = \frac{target\ height}{original\ height} \quad (5)$$

$$w\_ratio = \frac{target\ width}{original\ width} \quad (6)$$

- To prevent the image from being stretched or compressed unevenly, the smallest scaling ratio between the height and width should be selected. This ensures that the image is proportionally resized and no dimension exceeds the target size:

$$scale\_factor = (h\_ratio, w\_ratio) \quad (7)$$

- Based on the selected  $scale\_factor$ , the new image dimensions can be calculated to adjust proportionally both the height and width according to the following chosen ratio:

$$n\_height = o\_height * scale\_factor \quad (8)$$

$$n\_width = o\_width * scale\_factor \quad (9)$$

where  $o\_height$  and  $n\_height$  are the original and new heights of the image, and  $o\_width$  and  $n\_width$  are the original and new widths of the DICOM image, respectively.

As mentioned above, the dataset contains images of various sizes from different mammography machines. Using a standard cropping and resizing method, some images may have white padding after resizing and may not accurately capture the breast region. With the proposed cropping method, the process is automated, ensuring that the cropped images accurately match the desired breast region without unnecessary background.

### 3) Image Augmentation

Image augmentation is a popular technique to enhance the diversity and balance of training data. Using balanced datasets to train DL networks results in higher classification performance. Image augmentation can generate more images from the original ones without collecting additional images. In practice, common augmentation techniques include rotation, flipping, cropping, and others. Applying augmentation techniques can make the model more generalized, reduce overfitting, as well as improve performance on test data.

### E. Deep Learning for Breast Cancer Classification

This study used the ResNet50 DL model to classify BC. ResNet50 consists of 50 deep layers, with its main components being residual blocks, where each block contains convolutional layers, batch normalization layers, and the ReLU activation function. The network structure is divided into five main stages, each consisting of multiple convolutional and pooling layers, enabling the model to learn complex features from the input data. The stages are described as follows:

- Conv1:** The first convolutional layer has a  $7 \times 7$  filter with a stride of 2 to reduce the size of the input image and capture general features. Following this, a  $3 \times 3$  max pooling layer is applied to further decrease the data dimensions.
- Conv2-Conv5:** These stages consist of multiple bottleneck residual blocks, each containing three consecutive convolutional layers with filter sizes of  $1 \times 1$ ,  $3 \times 3$ , and  $1 \times 1$ , respectively. The first  $1 \times 1$  layer reduces the number of channels in the input data and minimizes the number of parameters for computation. The  $3 \times 3$  layer performs the main convolution operation and extracts important spatial features. The final  $1 \times 1$  layer restores the number of channels to match the expected output dimensions and also ensure compatibility with the rest of the network, as described in Figure 2.

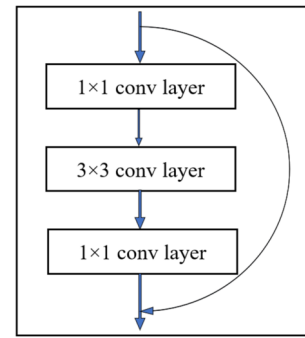


Fig. 2. The bottleneck residual block in the ResNet50 architecture.

## III. RESULTS AND DISCUSSION

The proposed system's performance was evaluated using the VinDr-Mammo BC image dataset [14].

### A. DICOM Image Preprocessing Results

The VinDr-Mammo BC image dataset contains numerous DICOM images with varying sizes and diverse breast region positions. Therefore, the DICOM images need to be preprocessed to extract the most distinct breast regions to train the deep learning network for BC classification. BC images were segmented using the Otsu method combined with thresholding. Next, the contours method was applied to identify objects within the images. Finally, a bounding box was generated around the breast region of each image, and the extracted breast region was cropped for classification. Figure 3 illustrates the segmentation process using Otsu, object boundary detection with contours, and the identification of the breast region using a bounding box.

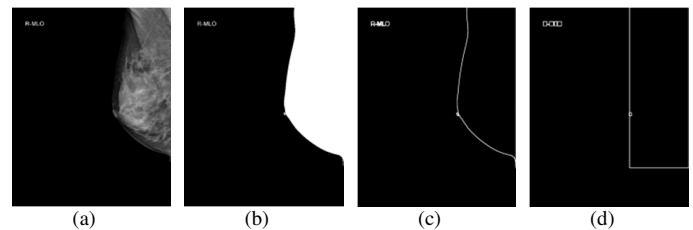


Fig. 3. DICOM image preprocessing results: (a) original image, (b) segmentation process using Otsu, (c) boundary with object contours, (d) bounding box.

Figures 4 and 5 present the results of image cropping and resizing to  $512 \times 512$ . Figure 6 shows cases where the breast parts in an image are positioned on the left and right, while Figure 5 represents cases of the breasts positioned diagonally at the upper left and upper right. The results indicate that in all these cases, the cropping and resizing process effectively preserves the breast regions, ensuring high-quality outputs.

In addition, the dataset includes special cases where images have black-and-white backgrounds, as shown in Figure 6. In these cases, the image cropping algorithm still produces good results. The preprocessing results show that all images, regardless of breast position and size, can be accurately cropped to extract the necessary breast region and resized to  $512 \times 512$ .

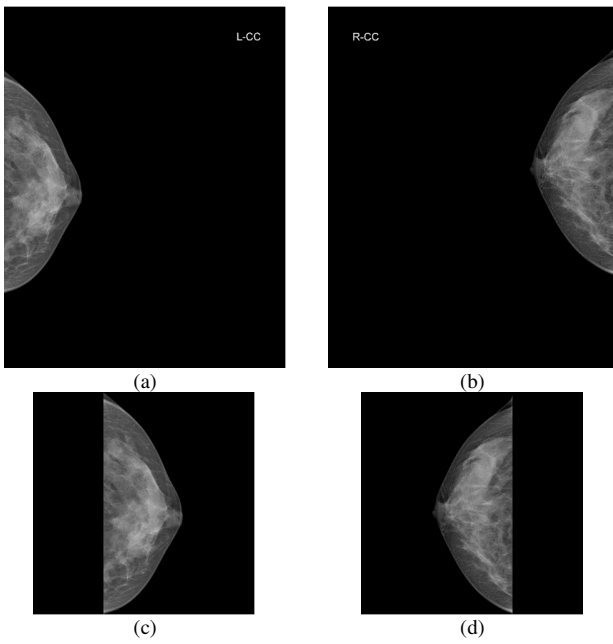


Fig. 4. Representation of the small-sized breast cancer images located on the left and right sides: (a) and (b) Original images, (c) and (d) images after cropping and resizing to 512x512.

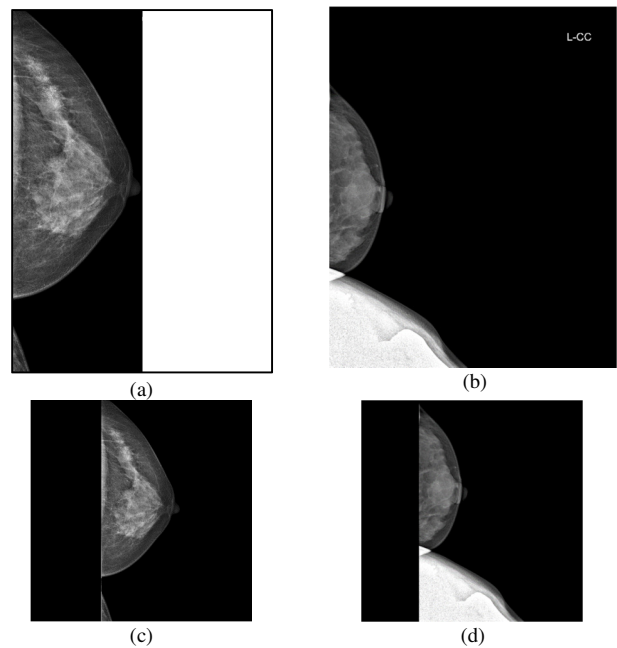


Fig. 6. Representation of the breast cancer images with some special cases: (a) and (b) original images, (c) and (d) images after cropping and resizing to 512x512.

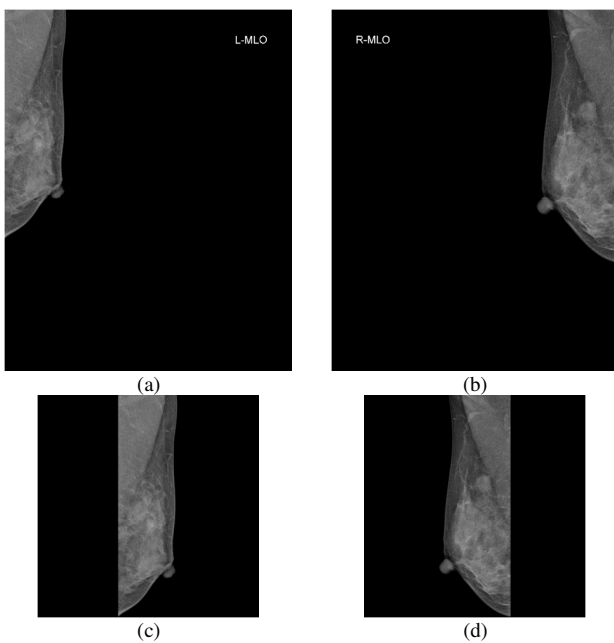


Fig. 5. Representation of the small-sized breast cancer image positioned diagonally in the top left and top right corners: (a) - (b) Original images, (c) - (d) images after cropping and resizing to 512x512.

**B. Breast Cancer Classification result**

The dataset has a significant imbalance in the number of images across classes. In particular, the number of images in classes 2 and 4 is 212 and 18,232, respectively. Therefore, data augmentation is essential to improve classification performance. Image augmentation involved vertical and horizontal flipping and image rotation within the range of  $\pm 50^\circ$ .

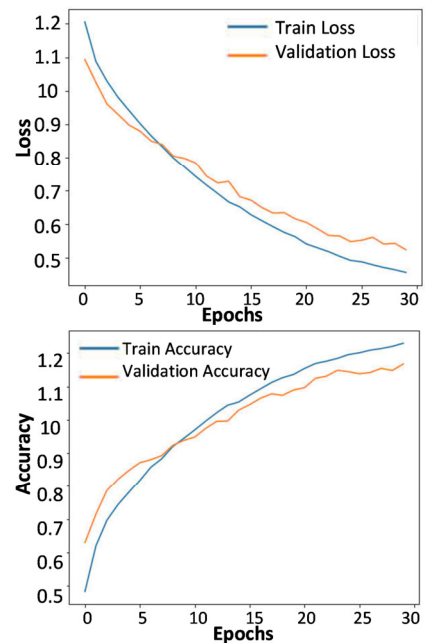


Fig. 7. Training results for Case 3 (10,000 images per class).

Four experimental scenarios were tested: In Case 1, each class contains 2,000 images, in Case 2, each class contains 5,000 images, in Case 3, each class contains 10,000 images, and in Case 4, each class contains 10,000 images, except for class 4, which retains 18,232 images. For class 4, a random selection was applied to match the number of images in the other classes. The total dataset was split into 80% for training, 10% for validation, and 10% for testing the model.

The ResNet50 model was used to classify BC images. The images were resized to be 512×512 and trained the network for 30 epochs. Figure 7 presents the training results for Case 3, where the number of processed images per class is 10,000. The results show that the loss continuously decreased and the accuracy improved significantly as the number of epochs increased. Figure 8 presents the confusion matrix for Case 3, in which the classification performance for the Calcification category is excellent. However, the classification performance for the Mass category is lower.

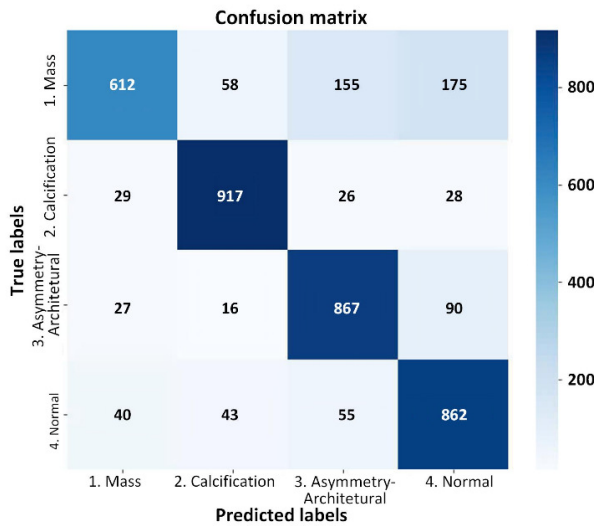


Fig. 8. Confusion matrix for Case 3 (10,000 images in each class).

Based on the confusion matrix results, evaluation metrics such as Accuracy (Acc), Precision (Pre), Recall (Rec), and F1-score (F1s) were calculated to evaluate the classification performance across different classes [15]. Figure 8 presents the confusion matrix results for Case 3, where it can be seen that the classification performance across all classes is relatively good. In particular, the Calcification category had the highest classification accuracy of 92%, while the Mass category had an accuracy of 61%. Table III summarizes the image classification results for Case 3.

TABLE III. RESULTS FOR BREAST CANCER CLASSIFICATION

Class	Label	Acc	Pre	Rec	F1s
1	Mass	0.61	0.86	0.61	0.72
2	Calcification	0.92	0.89	0.92	0.90
3	Architectural-Asymmetry	0.87	0.79	0.87	0.82
4	Normal	0.86	0.75	0.86	0.80

Table VI presents the comparative performance results of the four cases. In Case 1, where the number of images per class was augmented to 2,000, classification performance was the lowest, with results for Acc, Pre, Rec, and F1s of 72.92%, 75.64%, 72.92%, and 70.66%, respectively. As the number of augmented images increased, the classification performance improved. In practice, Acc reached 77.83% when the number of images increased to 5,000 and 81.45% when it increased to 10,000. However, in Case 4, since the number of images in the

Normal class was 18,232, the classification performance decreased when increasing the number of images in the Mass, Calcification, and Architectural and Asymmetry classes to 10,000. In this case, the results were Acc=81.65%, Pre=84.14%, Rec=78.41%, and F1s=79.95%. These results indicate that the classification performance across different classes was inconsistent, leading to performance discrepancies between classes.

TABLE IV. PERFORMANCE COMPARISON FOR THE FOUR CASES

	Case 1	Case 2	Case 3	Case 4
Acc	72.92	77.83	81.45	81.65
Pre	75.64	77.80	82.09	84.14
Rec	72.92	77.84	81.45	78.41
F1s	70.66	77.82	81.07	79.95

DL has been widely applied for classification in various domains, including agriculture, healthcare, aviation, and industry. In the medical field, DL is increasingly utilized for early diagnosis, disease classification, and other applications. For BC classification, the ResNet50 deep learning model has been employed with promising results [16-18]. In particular, in [16] ResNet50 was applied for BC classification on the BreakHis open dataset, achieving a high accuracy of 92.24%, but this system was limited to distinguishing between benign and malignant tumor types. In [17], ResNet50 used a self-collected breast cancer dataset consisting of 2,088 images classified into Healthy and Sick categories, achieving an accuracy of more than 80% [17]. This study applied ResNet50 to classify four different subtypes of BC, achieving an accuracy of 81.45%.

The VinDr-Mammo dataset consists of BC images collected from Vietnamese patients. Since this is a relatively new dataset, there are limited studies on it. Research on the VinDr-Mammo could provide valuable support for BC diagnosis in Vietnam. Moreover, this study serves as a foundation for developing more advanced algorithms to enhance BC detection and classification in the country. This study proposes a combination of DICOM image preprocessing and the ResNet DL model to classify different BC subtypes using this dataset. The results indicate that increasing the number of images per class to 10,000 improves classification performance. However, when the Normal class remains at 18,232 images, the classification performance across different classes is still suboptimal. Future research will aim to expand the dataset and enhance deep learning models to further improve classification performance. This study could serve as a basis for scientists to develop algorithms to improve BC detection and classification.

#### IV. CONCLUSION

Early and accurate diagnosis of BC can significantly improve patient recovery outcomes. This study combined an automatic image segmentation method with DL for BC classification in DICOM images. The experimental results demonstrated that the proposed method is well-suited for this purpose. In particular, when data augmentation was applied to increase the number of images per class to 10,000, classification performance improved significantly, achieving

Acc=81.45%, Pre=82.09%, Rec=81.45%, and F1s=81.07%. However, due to the imbalance in the number of images across different classes, the classification performance for certain classes remained lower, requiring further augmentation of the underrepresented classes. This research on BC detection and classification using the VinDr-Mammo dataset can serve as a foundation for scientists to develop further studies using this dataset. In the future, larger and more diverse datasets will be explored and integrated to create a more balanced dataset for improving BC detection and classification.

#### ACKNOWLEDGMENT

This work is supported by Ho Chi Minh City University of Technology and Education (HCMUTE) under Grant No. T2024-133.

#### REFERENCES

- [1] J. Kim *et al.*, "Global patterns and trends in breast cancer incidence and mortality across 185 countries," *Nature Medicine*, vol. 31, no. 4, pp. 1154–1162, Apr. 2025, <https://doi.org/10.1038/s41591-025-03502-3>.
- [2] A. Elhusseiny, "Women's cancer is getting worse in Asia Pacific," *World Economic Forum*, Oct. 11, 2023. <https://www.weforum.org/stories/2023/10/womens-cancer-is-getting-worse-in-asia-pacific-heres-what-to-do/>.
- [3] VnExpress, "Novartis sponsors expert talkshow to raise breast cancer awareness - VnExpress International," *VnExpress International*. <https://e.vnexpress.net/news/business/novartis-sponsors-expert-talkshow-to-raise-breast-cancer-awareness-4544893.html>.
- [4] L. C. V. Priya, V. G. Biju, B. R. Vinod, and S. Ramachandran, "Deep learning approaches for breast cancer detection in histopathology images: A review," *Cancer Biomarkers*, vol. 40, no. 1, pp. 1–25, May 2024, <https://doi.org/10.3233/CBM-230251>.
- [5] B. Asadi and Q. Memon, "Efficient breast cancer detection via cascade deep learning network," *International Journal of Intelligent Networks*, vol. 4, pp. 46–52, Jan. 2023, <https://doi.org/10.1016/j.ijin.2023.02.001>.
- [6] S. M. Shaaban, M. Nawaz, Y. Said, and M. Barr, "An Efficient Breast Cancer Segmentation System based on Deep Learning Techniques," *Engineering, Technology & Applied Science Research*, vol. 13, no. 6, pp. 12415–12422, Dec. 2023, <https://doi.org/10.48084/etasr.6518>.
- [7] D. Albashish, R. Al-Sayyed, A. Abdullah, M. H. Ryalat, and N. Ahmad Almansour, "Deep CNN Model based on VGG16 for Breast Cancer Classification," in *2021 International Conference on Information Technology (ICIT)*, Amman, Jordan, Jul. 2021, pp. 805–810, <https://doi.org/10.1109/ICIT52682.2021.9491631>.
- [8] S. Shamy and J. Dheeba, "A research on detection and classification of breast cancer using k-means GMM & CNN algorithms," *International Journal of Engineering and Advanced Technology*, vol. 8, no. 6S, pp. 501–505, 2019.
- [9] V. S. Vijayan and P. L. Lekshmy, "Deep learning based prediction of breast cancer in histopathological images," *International Journal of Engineering Research & Technology*, vol. 8, no. 07, pp. 148–152, 2019.
- [10] N. Wu *et al.*, "Deep Neural Networks Improve Radiologists' Performance in Breast Cancer Screening," *IEEE Transactions on Medical Imaging*, vol. 39, no. 4, pp. 1184–1194, Apr. 2020, <https://doi.org/10.1109/TMI.2019.2945514>.
- [11] A. Khalid *et al.*, "Breast Cancer Detection and Prevention Using Machine Learning," *Diagnostics*, vol. 13, no. 19, Jan. 2023, Art. no. 3113, <https://doi.org/10.3390/diagnostics13193113>.
- [12] Z. Zhu, Y. Sun, and B. Honarvar Shakibaei Asli, "Early Breast Cancer Detection Using Artificial Intelligence Techniques Based on Advanced Image Processing Tools," *Electronics*, vol. 13, no. 17, Jan. 2024, Art. no. 3575, <https://doi.org/10.3390/electronics13173575>.
- [13] Z. Wang *et al.*, "Breast Cancer Detection Using Extreme Learning Machine Based on Feature Fusion With CNN Deep Features," *IEEE Access*, vol. 7, pp. 105146–105158, 2019, <https://doi.org/10.1109/ACCESS.2019.2892795>.
- [14] H. H. Pham, H. Nguyen Trung, and H. Q. Nguyen, "VinDr-Mammo: A large-scale benchmark dataset for computer-aided detection and diagnosis in full-field digital mammography," *PhysioNet*, <https://doi.org/10.13026/BR2V-7517>.
- [15] T. N. Nguyen, T. H. Nguyen, M. H. Nguyen, and S. Livatino, "Wavelet-Based Kernel Construction for Heart Disease Classification," *AEEE Advances in Electrical and Electronic Engineering*, vol. 17, no. 3, pp. 306–319, Sep. 2019, <https://doi.org/10.15598/aeee.v17i3.3270>.
- [16] N. Behar and M. Shrivastava, "ResNet50-Based Effective Model for Breast Cancer Classification Using Histopathology Images," *CMES - Computer Modeling in Engineering and Sciences*, vol. 130, no. 2, pp. 823–839, Dec. 2021, <https://doi.org/10.32604/cmcs.2022.017030>.
- [17] S. Malathi, "Breast Cancer Detection With Resnet50, Inception V3, And Xception Architecture.," *Journal of Pharmaceutical Negative Results*, vol. 14, no. 4, pp. 60–68, 2023.
- [18] E. Al. T. Sunil Kumar, "Breast Cancer Classification and Predicting Class Labels Using ResNet50," *Journal of Electrical Systems*, vol. 19, no. 4, pp. 270–278, Jan. 2024, <https://doi.org/10.52783/jes.638>.